

# Design and evaluation of a mucoadhesive gel-forming spray for local delivery of betamethasone sodium phosphate in aphthous ulcer management

Mawadda B. Al-Juboori<sup>1</sup>, Eman B. H. Al-Khedairy<sup>1</sup>

<sup>1</sup> Department of Pharmaceutics, College of Pharmacy, University of Baghdad, Baghdad, Iraq

Corresponding author: Mawadda B. Al-Juboori (Muda.abd2200@copharm.uobaghdad.edu.iq)

Received 14 May 2025 ♦ Accepted 22 July 2025 ♦ Published 16 October 2025

**Citation:** Al-Juboori MB, Al-Khedairy EBH (2025) Design and evaluation of a mucoadhesive gel-forming spray for local delivery of betamethasone sodium phosphate in aphthous ulcer management. *Pharmacia* 72: 1–16. <https://doi.org/10.3897/pharmacia.72.e158871>

## Abstract

Mouth ulcers are common oral lesions. Although several topical treatments are commercially available, their limited residence time requires frequent application, which remains a significant drawback. This study aimed to develop a novel mucoadhesive, thermo-sensitive, in situ gel-forming spray for local delivery of betamethasone sodium phosphate, thereby reducing systemic exposure. Formulations were optimized using the design of experiment approach to investigate the effects of thermosensitive polymers (Poloxamer 407 and Poloxamer 188), mucoadhesive polymer (hyaluronic acid), and drug incorporation on gelation temperature and time. The optimized formulation gelled at  $33.3 \pm 0.7$  °C within  $14.79 \pm 1.87$  s and showed a spray angle of  $43.6 \pm 0.62^\circ$  at 3 cm (ovality ratio  $1.1 \pm 0.06$ ), indicating consistent plume formation. This formulation demonstrated uniform spray dose delivery of ~99% drug content per actuation and exhibited good mucosal biocompatibility in histological studies. These findings suggest that the proposed in situ gel-forming spray is a promising localized delivery system for the effective management of aphthous ulcers.

## Keywords

betamethasone sodium phosphate, design of experiment, gel-forming spray, hyaluronic acid, in situ gel

## Introduction

Oral ulcers, also known as aphthous ulcers, are painful breaks in the continuity of the oral epithelial tissue, which acts as a barrier to protect deeper tissue (Inchara and Uma Maheshwari 2020). They are brought about by several causes, including recurrent aphthous stomatitis, direct trauma (physical or chemical), adverse drug effects, infections, hematinic deficiency, and disorders of the immune system (Gurav and Husukale 2023). The population prevalence of aphthous ulcers is approximately 4%, and around

80% of patients undergoing radiotherapy also experience oral ulcers (Sanguansajapong et al. 2022). Betamethasone sodium phosphate (BSP) is a synthetic corticosteroid with potent glucocorticoid activity, primarily used for its strong anti-inflammatory properties (Vardanyan and Hruby 2006). It has a short circulation half-life and undesirable systemic side effects. Therefore, it is more favorable for local and sustained delivery (Zhang et al. 2017). Topical corticosteroids are typically considered the first-line treatment for mouth ulcers, and BSP 500 µg soluble tablets are commonly used as a mouth rinse (Medicines Information

Services 2022). Clinical studies have demonstrated that BSP has significant efficacy in reducing pain, lesion size, and duration in patients with recurrent aphthous ulcers, making it a suitable corticosteroid for topical treatment of oral ulcers (Alsaahaf et al. 2023).

However, corticosteroid mouth rinses have drawbacks. They contact the entire oral cavity, including both healthy and diseased areas. More importantly, there is an increased possibility of ingestion of the rinse if not spat out entirely. Given the high solubility of BSP and its rapid absorption through the gastrointestinal tract, this may result in unwanted systemic exposure (Rudralingam et al. 2017). Several forms of topical therapy can be used to manage mouth ulcers effectively. However, the drug's short retention time at the site of application should be addressed as a limitation to its therapeutic efficacy (Gurav and Husukale 2023). Formulating a mucoadhesive *in situ* gel (IG) that allows for more specific application and prolongs drug residence time at the application site could ensure greater therapeutic efficacy and help overcome these limitations (Li et al. 2020a).

Oral sprays are a popular form of local administration for treating oral cavity problems. A topical metered-dose spray is characterized by the presence of a dosing pump unit, which efficiently delivers an accurate therapeutic quantity of the drug to the intended site of action, ensuring minimal systemic exposure and optimizing local drug concentrations (Ranade et al. 2017). Gel-forming sprays are polymer-based formulations that are sprayable at room temperature and form a mucoadhesive gel upon contact with mucosal tissue (Li et al. 2020a). This can be achieved by using thermosensitive polymers, such as poloxamers, which are widely employed in drug delivery systems due to their amphiphilic nature, biocompatibility, and ability to undergo a phase transition at body temperature, making them ideal for IG formulations (Gurav and Husukale 2023). Since the IG is applied to the required site in spray form, this provides an effective technique to eliminate the risk of formulation cross-contamination, improve patient compliance, and reduce the frequency of application (Wong et al. 2021). Furthermore, mucoadhesive polymers in the formulation create a viscous gel that prolongs adhesion and retention time on the mucosal membrane, thereby ensuring an extended therapeutic effect (Maslii et al. 2024).

Hyaluronic acid (HA) is one of the most commonly used mucoadhesive polymers in the development of drug formulations for oromucosal applications (Wong et al. 2021). HA is a natural hydrophilic polymer that is biodegradable, biocompatible, and non-immunogenic. It contains reactive functional groups (e.g., carboxyl groups) that promote interaction with mucosal tissue (Karaküçük and Tort 2021). For example, JH Lee et al. demonstrated the efficacy and safety of HA gel in patients with recurrent oral ulcers, highlighting HA's therapeutic benefit in ulcer healing (Lee et al. 2008).

The use of response surface methodology is becoming an essential strategy in pharmaceutical development, enabling researchers to evaluate multiple formulation

variables simultaneously and propose the optimal combination of factors to yield the most effective product (Nurman et al. 2019). To optimize the IG formulations, we employed an optimal custom design (OCD) using design of experiment (DOE), aiming for formulations with a gelation temperature in the physiological range and a suitable gelation time. This design approach provides flexibility in selecting factor levels while minimizing the number of experimental runs (Fukuda et al. 2018).

This work aimed to develop a mucoadhesive sprayable solution that forms a gel at physiological temperature, enabling site-specific delivery of BSP to enhance and accelerate oral ulcer healing, while using HA to enhance formulation mucoadhesive properties. An OCD model was used to generate optimized formulations, which were further evaluated for oromucosal spray properties.

## Materials and methods

### Materials

Betamethasone sodium phosphate was purchased from Leyan (Shanghai Haohong Biopharmaceutical Technology Co., Ltd.); Poloxamers 407 and 188 grades from Baoji Guokang Bio-Technology Co., Ltd.; hyaluronic acid as sodium hyaluronate salt (molecular weight: 8000–15000 Da) from Bide Pharmatech Co., Ltd.; benzalkonium chloride 80% from McLean Biochemical Technology Co., Ltd.; mucin from porcine (Saitonc<sup>®</sup>, Beijing Jinming Biotechnology Co., Ltd.); and dialysis membrane with 14000 Da molecular weight cut-off from Shanghai Dianrui Biotechnology Co., China. Spray containers were purchased from Vipolishtry (Amazon.co.uk).

### Preparation of oral IG formulations

The thermosensitive IG formulations were prepared using the cold method by slowly adding predetermined amounts—established based on a preliminary study—of Poloxamer 407 (P407, 18–20%) alone or combined with Poloxamer 188 (P188, 1–2%) to cold deionized water (DW) with gentle stirring at 500 rpm. The resulting dispersion was then refrigerated at 4 °C for 24 h to allow complete hydration of the poloxamers. Afterward, the mucoadhesive polymer HA (0–1%) and benzalkonium chloride (0.01%) were introduced to the formulations with gentle agitation until a clear solution was obtained (Alabdly and Kassab 2023). To investigate the impact of drug loading on sol–gel transition temperatures, each formulation was prepared twice: one with the addition of BSP and the other without (blank). BSP was incorporated at a concentration of 0.33% (w/v), selected based on preliminary spray actuation volume measurements to deliver approximately 0.5 mg of drug per spray. This dose was chosen to align with clinical topical corticosteroid use in aphthous ulcer management and to improve patient compliance while minimizing systemic exposure.

## Experimental design

Design-Expert 13 software (version 13.0.5.0, Stat-Ease, USA) was used to optimize IG formulations. The OCD design employed the D-optimal model to assess the relationship between the independent factors (design factors) at different levels and the dependent variables (experiment responses), as shown in Table 1. The three design factors were (A) P407% at three levels, (B) P188% at three levels, and (C) HA % at five levels, whereas the experiment responses were ( $Y_1$ ) gelation temperature without drug (blank), ( $Y_2$ ) gelation temperature with drug, and ( $Y_3$ ) gelation time, resulting in 27 experimental runs as detailed in Table 2.

**Table 1.** Design independent variables and their levels.

| Factors | Parameters | Levels                |
|---------|------------|-----------------------|
| A       | P407%      | 18, 19, 20            |
| B       | P188%      | 0, 1, 2               |
| C       | HA %       | 0, 0.25, 0.5, 0.75, 1 |

**Table 2.** The OCD experiment runs and the responses.

| Runs | A: P407 (%) | B: P188 (%) | C: HA (%) | $Y_1$ : Gelation temperature without drug (°C) | $Y_2$ : Gelation temperature with drug* (°C) | $Y_3$ : Gelation time (s) |
|------|-------------|-------------|-----------|--|--|---------------------------|
| 1    | 20          | 0           | 0         | 25.6   | 25.6   | 7.76                      |
| 2    | 20          | 1           | 0.75      | 24.9   | 28.3   | 10.89                     |
| 3    | 20          | 1           | 0.75      | 25.3   | 29   | 9.47                      |
| 4    | 20          | 2           | 1         | 28.7   | 35.8   | 37.4                      |
| 5    | 20          | 2           | 0.75      | 29.9   | 33.8   | 25.74                     |
| 6    | 20          | 2           | 0.5       | 30.7   | 33   | 20.78                     |
| 7    | 20          | 2           | 0.25      | 31.7   | 32.3   | 11.53                     |
| 8    | 19          | 0           | 0.75      | 27.2   | 29.3   | 11.05                     |
| 9    | 19          | 0           | 0.75      | 26.2   | 28.2   | 16.92                     |
| 10   | 19          | 0           | 0.25      | 27.5   | 28.1   | 10.31                     |
| 11   | 19          | 1           | 1         | 27.1   | 32.7   | 40.1                      |
| 12   | 19          | 1           | 0.25      | 29.6   | 30.1   | 7.08                      |
| 13   | 19          | 1           | 0.25      | 30.2   | 30.7   | 15.3                      |
| 14   | 19          | 1           | 0.25      | 29.1   | 30.5   | 12.2                      |
| 15   | 19          | 2           | 1         | 31.9   | 38.6   | 40.31                     |
| 16   | 19          | 2           | 0.25      | 33.5   | 34.7   | 20.86                     |
| 17   | 19          | 2           | 0         | 35.4   | 35.4   | 41.44                     |
| 18   | 18          | 0           | 0.75      | 25.9   | 31.3   | 16.81                     |
| 19   | 18          | 0           | 0.25      | 27.2   | 28.1   | 11.01                     |
| 20   | 18          | 1           | 1         | 28.6   | 34.6   | 40.25                     |
| 21   | 18          | 1           | 0.75      | 29.3   | 33.5   | 20.58                     |
| 22   | 18          | 1           | 0.25      | 30.3   | 33.8   | 13.81                     |
| 23   | 18          | 1           | 0         | 29.6   | 29.6   | 28.42                     |
| 24   | 18          | 2           | 0.75      | 34.7   | 37.9   | 19.43                     |
| 25   | 18          | 2           | 0.75      | 33.3   | 36.8   | 15.01                     |
| 26   | 18          | 2           | 0.25      | 35.7   | 36.3   | 10.21                     |
| 27   | 18          | 2           | 0         | 35.9   | 35.9   | 43.5                      |

\* BSP concentration was 0.33% w/v based on preliminary evaluation of spray actuation volume.

## Determination of sol–gel transition temperature and gelling time

The gelation temperature is defined as the temperature at which the phase transition occurs from the flowable liquid phase (sol) to the stiff and flow-resistant semisolid

phase (gel). The test tube inversion method was used to determine the gelation temperature of the formulations (Fig. 1). One milliliter of each preparation (with and without the drug) was placed in a test tube and incubated in a water bath maintained at  $20 \pm 0.5$  °C (Obayes and Thomas 2025). The water bath temperature was increased gradually by 1 °C every 2 minutes. Before each temperature increment, the test tube was inverted to check the formulation's flowability, and the temperature at which the formulation ceased to flow upon inversion was recorded as the gelation temperature. Furthermore, the gelation time—defined as the time required for a complete transition from sol to gel—was also determined using the tube inversion method. The tube containing 1 mL of each preparation was placed in a preheated water bath at 37 °C and inverted every 10 seconds. The elapsed time until the gel no longer flowed was recorded as the gelation time (Hamzah and Kassab 2024).

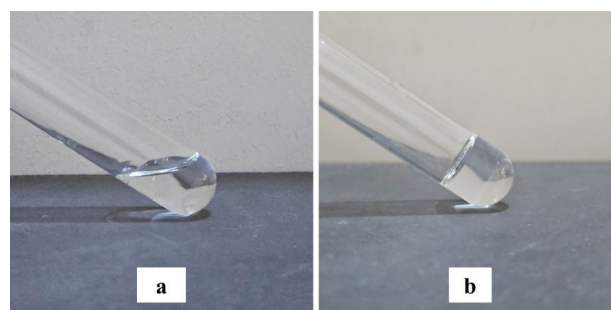


**Figure 1.** The test tube inversion method at room temperature (a) and after the sol–gel transition temperature (b).

## Drug–excipient compatibility study

The compatibility study was carried out using Fourier-transform infrared (FTIR) spectroscopy. The FTIR spectra of pure BSP, poloxamers, HA, and the physical mixture (PM) of BSP and polymers combined were scanned in the range of 1400–400  $\text{cm}^{-1}$  wavenumber. The spectra were compared to detect any interactions between the drug and polymers (Raheema and Kassab 2022).

## Optimization of oral IG formulations

The DOE applied a desirability function to convert each response into a dimensionless desirability score, ranging from 0 (least desirable) to 1 (most desirable) (Al-Sawaf and Jalal 2023). Optimization criteria were targeted to obtain BSP-loaded formulations with optimal gelation temperatures and minimal gelation times, ensuring fast gelation at physiological temperature. The responses  $Y_2$  and  $Y_3$  were assigned to a specific goal: minimizing the gelation temperature (33–35 °C) and shortening the gelation time (7–15 s). Seven formulations with a desirability score of 1 (F1–F7), each with varying polymer compositions, were selected for further evaluation.

## Characterizations of optimized formulations

### Appearance and pH evaluation

Visual examination was employed to assess the clarity of formulas and the presence or absence of any aggregations in the physical appearance. The pH was determined using a digital pH meter (Hanna Instruments, Italy), where the pH meter probe was immersed in each formulation for 5 minutes (Sulaiman et al. 2018).

### Gelling capacity

The gelling capacity is based on the retention time of the formed gel in a specific environment. A blue coloring agent was used to impart color to the formulas, aiding in visual assessment (Fig. 2). A drop from the formula was then placed into a glass tube containing 2 mL of freshly prepared buffer solution with a pH of 6.8, equilibrated at  $37 \pm 1$  °C, and observed visually every 15 minutes for complete dissociation of the gel (Raheema and Kassab 2022).

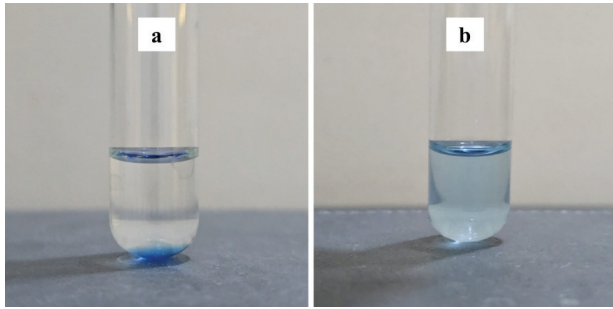


**Figure 2.** Gelling capacity assessment using a coloring agent: **a.** Immediate gel formation upon addition into buffer solution at  $37 \pm 1$  °C, and **b.** After complete gel dissolution.

### Viscosity study

The viscosity measurements of optimized formulations were carried out using a digital viscometer NDJ-5S (Drawell, China). Spindle no. 1 was used at room temperature ( $25 \pm 1$  °C), and spindle no. 4 was used at physiological temperature ( $37 \pm 1$  °C), under different shear rates (6, 12, 30, and 60 rpm). The spindle was immersed in the sample and allowed to rotate for 1 minute before viscosity was recorded (Alkufi and Kassab 2019).

## Texture profile analysis

Texture profile analysis (TPA) was used to determine the mechanical properties of the prepared gels using a TA-XT Plus Texture Analyzer (Stable Micro Systems). A specific amount of each sample was transferred into a 10 mL beaker and measured at room temperature (liquid state) and at  $37 \pm 1$  °C for gel formation. The samples were then subjected to a double compression cycle using a stainless steel analytical probe (10 mm diameter) at 10 mm/s (test speed), with a predetermined depth of 15 mm and a delay period of 15 seconds between the end of the first compression and the beginning of the second (Fig. 3a). The obtained results provided the following mechanical properties: hardness (maximum force reached during the first compression, in grams), compressibility (the work required to deform the sample during the first compression, in g-s), adhesiveness (the work required to overcome the attractive forces between the sample and probe surfaces, in g-s), and cohesiveness (the work required for the sample surface to reunite with the probe surface, dimensionless) (Desai et al. 2022).

## Mucoadhesion analysis

The TA-XT Plus Texture Analyzer (Stable Micro Systems) was used to measure the mucoadhesive force of IG formulations. Mucin disks were used as a mucosal substrate and prepared by direct compression of crude porcine gastric mucin using a 15 mm diameter die, with a manual compression force held for 30 seconds. The mucin disk was attached with double-sided tape to the end of a flat circular probe (20 mm diameter). Immediately before testing, the mucin disk was hydrated by dipping it in a 5% (w/v) mucin solution for 30 s. Five milliliters of each optimized gel formulation were placed on a flat petri dish (6 cm diameter), maintained at  $37 \pm 1$  °C, and positioned under the probe. A force of 5 g was applied to the surface of the gel and maintained for 30 s (contact time); then, the probe was elevated at a speed of 10 mm/s (Fig. 3b). The obtained results measured the maximum required force for detachment in grams ( $F_{adh}$ ) and the work of adhesion in g-s ( $W_{adh}$ ), which corresponds to the area under the force-time curve (Bassi da Silva et al. 2018).

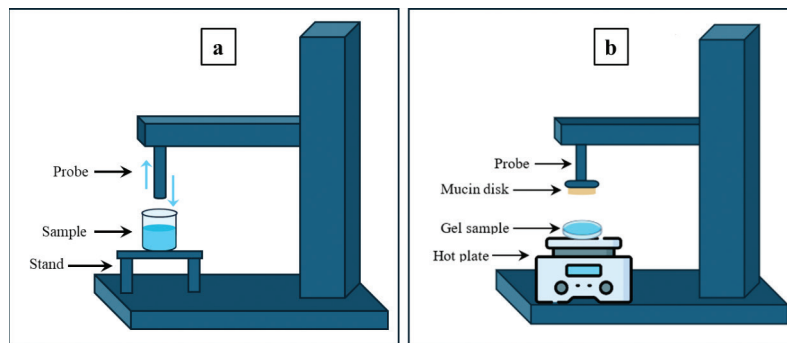


**Figure 3.** Illustration of the texture analyzer setup during **a.** TPA and **b.** The mucoadhesion test.

## Spray performance assessment

The spray delivery was evaluated for all optimized formulas using an amber glass spray container. A 30 mL spray container with a swiveling actuator (6.6 cm nozzle length) was used, which is considered suitable for oral cavity applications. Fig. 4a is a representative image of the spray and its components. A control formula was prepared by simply dissolving the BSP in water and was used to evaluate the effect of formulation excipients and their viscosity on spray characterizations.

## Spray angle measurement

To accurately measure the spray angle, two sheets of white paper were positioned at a 90° angle. One sheet was placed horizontally, where the sprayed sample would land, and the other was positioned vertically (beside it), supported by a stand. The height from the spray nozzle to the horizontal paper was marked. The colored sample solution was sprayed from specified distances of 3 cm and 6 cm to create a distinct pattern on the horizontal paper, where a half-circle was drawn around the sprayed product (Fig. 4b). Both a protractor and a spray angle formula were used to determine the correct spray angle (Hegde et al. 2025).

$$\theta = 2 \tan^{-1} \left( \frac{r}{l} \right)$$

Where  $\theta$ : spray angle,  $r$ : radius of spray pattern,  $l$ : nozzle height.

Studies have suggested that a spray angle of less than 85° is considered optimal for oral spray formulations, as it ensures efficient actuation while maximizing the coverage area (Angsusing et al. 2025).

## Spray pattern and ovality ratio

The imprint of the spray plume was visually determined after spraying once onto graph paper. The spray plume was evaluated by its maximum diameter (Dmax), minimum diameter (Dmin), and ovality ratio (Dmax/Dmin). The ovality ratio provides insight into spray shape and uniformity after actuation, where values near 1 signify a uniform circular pattern, whereas values greater than 1.5 represent an irregular (elliptic) shape. The evaluation of the spray pattern was performed at two heights (3 cm

and 6 cm) from the spray nozzle, as recommended by the Food and Drug Administration (FDA) regulations (Dedhiya and Economou 2002).

## Automated spray actuation evaluation

The FDA recommends the use of automated machines to measure the actuation force and pump weight of sprays, thereby eliminating variations due to analysts' hand spraying. A Universal Testing Machine (HZ-1007A, Dongguan Lixian Instrument Scientific Co., Ltd., China) was set with a pre-speed of 1 mm/s, a test speed of 8.333 mm/s, a preload of 0.5 kg, and a test direction of down, with a break judgment of 0.5%. The actuation parameters measured included the actuation force, which is the force required to initiate spraying, and the maximum force, which is the maximum force needed to perform complete actuation of the spray. Both were measured in kg.f. In addition, the plume weight of each optimum formula was measured by determining the weight of each dismissed shot unit from the spray after automated actuation and repeated ten times ( $n = 10$ ) to evaluate individual weight divergence (Doughty et al. 2011).

## Spray delivery profile (delivered dose uniformity)

A sequential spray delivery profile comprises three segments based on the determination of spray shot weight. Initially, priming actuations represent the number of actuations required to reach the intended uniform shot weight of the spray. Then, a relatively uniform shot weight is achieved, known as the stage of in-use actuations, which continues until the spray volume is exhausted (tail-off). All shot weights were determined using an electrical balance (Kern and Sohn GmbH, Germany). The spray container of each optimum formula was filled with 15.1 g of formula and weighed before the start of the sequential actuations. The weight of each shot was determined between every single actuation during the priming, in-use, and tail-off phases. The weight loss for each formulation was also determined after completion of the spray exhaustion phase, measured by the difference between the initial weight of the spray formulation before actuations and the remaining weight after the test was finished (Bastos et al. 2024).

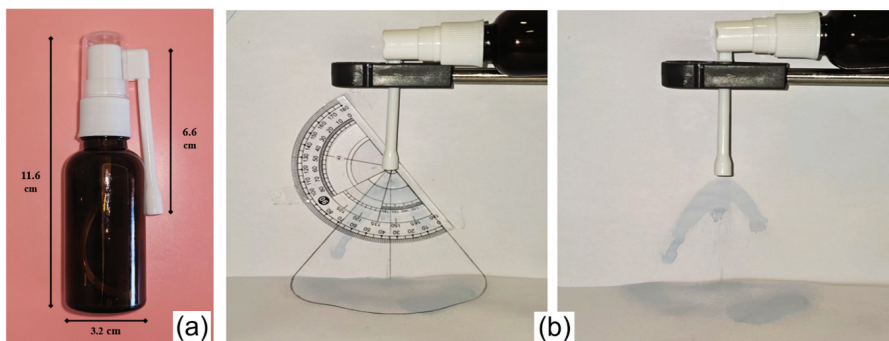


**Figure 4.** a. Image of the sprays used in this study and b. The spray angle calculation assembly.

### Drug content per each spray actuation

To measure the spray volume, the density of formulations needed to be calculated first. The weight of 1 mL of the optimum formula was accurately measured, and an average of ten weights was taken. The density was then calculated from the following equation:

$$\text{Density} = \frac{\text{Average weight}}{1\text{mL}}$$

The volume of actuation was obtained by taking the weight of ten actuations of the previously primed spray device. The following equation was then employed (Li et al. 2020b):

$$\text{Spray actuation volume} = \frac{\text{Weight of ten spray shots}}{10 \times \text{Density}}$$

The BSP concentration was tailored to deliver 0.5 mg per single spray actuation, enhancing patients' compliance. Afterward, the drug content for each optimal spray formulation was determined by discharging one shot volume of the spray formulation into a 50 mL volumetric flask, and the volume was completed with DW. Then, BSP was estimated spectrophotometrically using a UV-visible spectrometer (Shimadzu, Japan) at a  $\lambda_{\text{max}}$  of 242 nm.

### In vitro release study

A vertical Franz cell with a dialysis membrane (14000 Da) was used to study the release behavior of the drug from optimal formulations. The dialysis membrane was presoaked for 24 h with phosphate buffer (pH 6.8) and then mounted between the donor and receptor compartments. In the donor compartment, a single actuation of spray was applied onto the dialysis membrane. The receptor compartment was filled with 25 mL of freshly prepared phosphate buffer (pH 6.8) and kept at  $37 \pm 0.5$  °C with a magnetic stirrer at 200 rpm. At predetermined time intervals, a 1 mL volume was withdrawn from the receptor medium and immediately substituted with an equal amount of fresh buffer pH 6.8 equilibrated at  $37 \pm 1$  °C. The samples were measured spectrophotometrically at a  $\lambda_{\text{max}}$  of 242 nm. The release of pure drug solution spray was also conducted under the same conditions (Swain et al. 2019). The similarity factor ( $f_2$ ) was calculated to compare the drug release profiles using the following equation.

$$f_2 = 50 \log \left\{ 100 \left[ 1 + \frac{1}{n} \sum_{t=1}^n (Rt - Tt)^2 \right]^{-0.5} \right\}$$

Where Rt and Tt are the cumulative percentages of BSP released at each time point for the reference and test formulations, respectively. The release profiles are considered different if the  $f_2$  value is lower than 50 (Muselík et al. 2021).

### Histological irritation study

Ethical approval was granted before conducting this study by the Ethical Committee of the College of Pharmacy, University of Baghdad (REC032433R), and the

principles of the Office International des Epizooties' (OIE) on animal ethics guidelines were followed during this research. Two male New Zealand White rabbits with body weights of 3–3.5 kg and similar ages were selected to conduct macroscopic and histological examination. One of the rabbits was treated as a negative control, receiving a placebo spray (without BSP). Meanwhile, the other received the optimum formula. The rabbits consumed food at least one hour prior to the start of the study, and food was restricted throughout the experiment, except that fluid consumption was permitted after one hour of applying the spray formulation. The selected spray formulation was applied to the oral mucosa once. Visual observations were conducted before spray application and at 1, 2, 6, and 24 h after to detect any adverse reactions, such as discoloration, sloughing, erythema, or bleeding. At the end of 24 h, animals were sacrificed, and the oral mucosa tissue was carefully removed. The oral mucosa was then fixed in 10% neutrally buffered formalin. It was further washed and dehydrated, then decalcified and embedded in paraffin, and stained using eosin and hematoxylin to be examined under a light microscope (Atoosh and Ghareeb 2024).

### Statistical analysis

The results in this research were expressed as the mean value of three measurements ( $n = 3$ )  $\pm$  standard deviation (SD). Statistical analysis was performed using analysis of variance (ANOVA), with  $p$ -values less than 0.05 considered statistically significant.

## Results and discussion

### Preparation and optimization of oral IG

The DOE investigated the effect of formulation-independent variables on the characteristics of the IG formulation. A total of 27 formulations were prepared based on OCD compositions (Table 2). The gelation temperature in both blank and BSP-loaded formulations, as well as the gelation time, was greatly influenced by even slight changes in polymer concentrations.

The quadratic model provided the best fit for all three responses and was found to be significant when  $p < 0.05$ . The lack of fit values was found to be insignificant, indicating the validity of the chosen model ( $p > 0.05$ ). Furthermore, all responses showed compatible predictive powers, as indicated by the closeness of their predicted  $R^2$  and adjusted  $R^2$  values (less than 0.2 difference), which demonstrates how well the model fits the data. Notably, an  $R^2$  value close to 1 implies an excellent fit. Based on the statistical model proposed, the study is considered significant. In addition, all responses had a sufficient value of adequate precision; a ratio greater than 4 is desirable, and the model can reliably predict the outcomes (Table 3).

**Table 3.** Model analysis parameters of response variables.

| Parameters                     | Y <sub>1</sub>    | Y <sub>2</sub>    | Y <sub>3</sub>    |
|--------------------------------|-------------------|-------------------|-------------------|
| <b>Model (Quadratic)</b>       | p < 0.0001        | p < 0.0001        | p < 0.0001        |
| <b>p-value</b>                 | (Significant)     | (Significant)     | (Significant)     |
| <b>Model Terms</b>             |                   |                   |                   |
| A                              | p < 0.0001        | p < 0.0001        | p = 0.0132        |
| B                              | p < 0.0001        | p < 0.0001        | p = 0.0003        |
| C                              | p < 0.0001        | p = 0.0002        | p = 0.0039        |
| AB                             | p = 0.0264        | p = 0.5565        | p = 0.0103        |
| AC                             | p = 0.1619        | p = 0.2965        | p = 0.5419        |
| BC                             | p = 0.2022        | p = 0.6123        | p = 0.0544        |
| A <sup>2</sup>                 | p = 0.0003        | p = 0.0632        | p = 0.1084        |
| B <sup>2</sup>                 | p < 0.0001        | p = 0.0138        | p = 0.5596        |
| C <sup>2</sup>                 | p = 0.3504        | p = 0.1166        | p < 0.0001        |
| <b>Lack of fit p-value</b>     | 0.7716            | 0.1108            | 0.2278            |
|                                | (non-significant) | (non-significant) | (non-significant) |
| <b>R<sup>2</sup></b>           | 0.9810            | 0.9556            | 0.9026            |
| <b>Adjusted R<sup>2</sup></b>  | 0.9709            | 0.9322            | 0.8511            |
| <b>Predicted R<sup>2</sup></b> | 0.9544            | 0.8610            | 0.7469            |
| <b>Adequate precision</b>      | 30.3029           | 23.4252           | 12.9030           |

### Effect of formulation variables on gelation temperature (Y<sub>1</sub>, Y<sub>2</sub>)

The results of the ANOVA for the quadratic model concerning responses Y<sub>1</sub> and Y<sub>2</sub> are shown in Table 3. The model is significant for both responses ( $p < 0.0001$ ); in the case of Y<sub>1</sub>, the significant model terms are A, B, C, AB, A<sup>2</sup>, and B<sup>2</sup> ( $p$ -values less than 0.05 indicate significant model terms). The relationship between gelation temperatures and formulation factors, based on coefficient values, can be predicted using the following equation.

$$Y_1 = 28.97 - 1.61A + 3.45B - 1.25C - 0.4877AB - 0.3232AC - 0.3057BC - 1.09A^2 + 1.42B^2 - 0.3103C^2$$

Concerning the gelation temperature of blank formulations, the negative coefficient values for A (P407) and C (HA) indicate that as the concentrations of P407 and HA increase, the temperature required for gelation decreases. In contrast, the positive value for B (P188) suggests that as its concentration increases, the gelation temperature also increases (Fig. 5). This is explained in previous literature by the entanglement of poloxamer micelles. As the P407 concentration increases, the ratio of hydrophobic polypropylene oxide (PPO) also increases, resulting in faster dehydration of micelles and easier aggregation at lower temperatures. At the same time, higher P188 concentrations mean a larger ratio of the hydrophilic polyethylene oxide (PEO). Concomitantly, the micelles are less entangled and require a higher critical micelle temperature to result in micelle aggregation and eventually gelation (Alkufi and Kassab 2019). The mucoadhesive polymer HA contains hydroxyl and carboxyl groups that interact with PEO blocks, facilitating the closer packing of micelles and thereby reducing the gelation temperature. HA displays an extraordinary capability to retain water and behaves as an expanded random coil occupying a large hydrodynamic volume. As a consequence, the presence of HA in poloxamer solutions can accelerate the desolvation of poloxamer chains, promoting micellar aggregation and thus reducing the sol-gel transition temperature (Mayol et al. 2014).

In the case of Y<sub>2</sub>, the significant model terms were A, B, C, and B<sup>2</sup>. The relationship between the gelation temperature of BSP-loaded formulations and the design factors, based on coefficient values, is shown in the following equation.

$$Y_2 = 30.90 - 2.01 A + 3.76B + 1.38C + 0.1928 AB - 0.3816 AC + 0.1907 BC - 0.7621 A^2 + 1.02 B^2 + 0.8563 C^2$$

Upon the addition of BSP to formulations, there is a significant increase in gelation temperatures with increasing HA concentration, as indicated by positive coefficient values. In contrast, gelation behavior with poloxamers remained unaffected compared with blank formulas (Fig. 5). Similar findings have been reported in the literature; the addition of water-soluble drugs, especially in salt form, may alter the hydration dynamics and the thermosensitive behavior of the system (Hsieh et al. 2020; Russo et al. 2022). This phenomenon can be attributed to the interaction of HA with the poloxamer micelles and the surrounding aqueous environment, which increases the gelation temperature. This may be due to the steric hindrance or altered hydration dynamics introduced by HA–BSP interactions, which interfere with micelle packing and network formation. In contrast, the addition of HA to poloxamers alone (without BSP) facilitates micellar aggregation and network formation at lower temperatures, thereby decreasing the gelation temperature. This contrasting behavior underscores the modulatory effect of drug–polymer interactions on the thermogelling behavior of poloxamer-based systems (Bakhrushina et al. 2023).

### Effect of formulation variables on gelation time (Y<sub>3</sub>)

The ANOVA analysis results of the quadratic model for response Y<sub>3</sub> were significant (Table 3). The significant model terms are A, B, C, AB, and C<sup>2</sup>. The gelation time is inversely proportional to P407 concentration. However, the addition of HA first reduced the gelation time (decreasing from 41.44 s in run 17 to 20.86 s in run 16). A further increase in HA concentration (to 1%) then prolonged the gelation time (40.31 s in run 15). Increasing P188 concentration (0% to 2%) caused prolonged gelation time, as seen in runs 23 and 27 (28.42 and 43.5 s, respectively) (Table 2, Fig. 6). These trends are also evident in the coefficient values that depict the effect of formulation factors on gelation time as follows:

$$Y_3 = 8.47 - 3.61 A + 5.78 B + 4.91 C + 4.75 AB + 1.13 AC - 3.92 BC - 3.33 A^2 + 1.14 B^2 + 25.81 C^2$$

When the concentration of P407 increases, the number of micelles formed also increases, and the micelles are readily packed; consequently, less time is required for gelation, as previously reported in the literature (Salih and Ghareeb 2021). Additionally, P188 acts as a gelation retarder due to its relatively higher

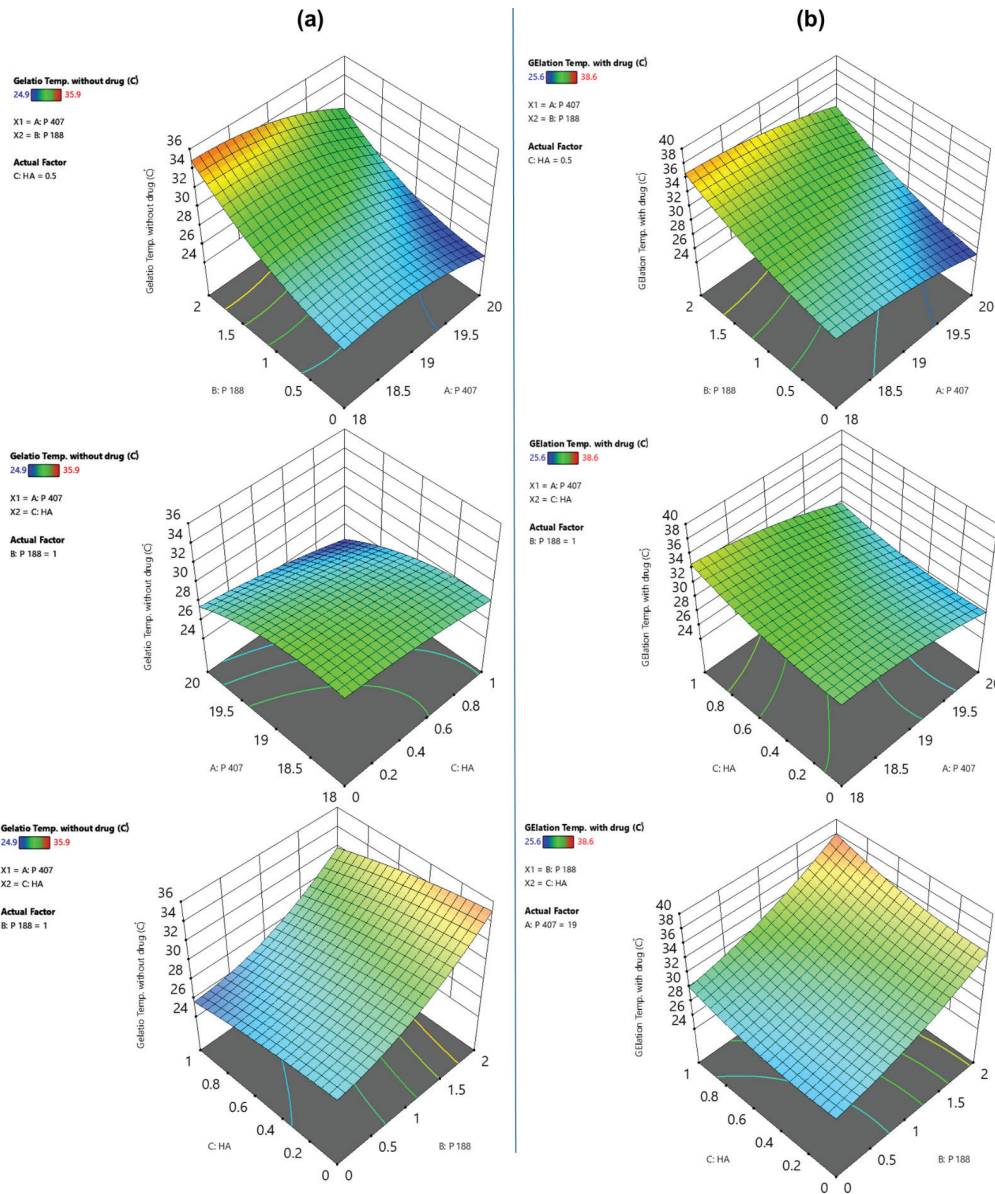


**Figure 5.** 3D response surface plots of **a.**  $Y_1$ , gelation temperature without drug (blank formulation), and **b.**  $Y_2$ , gelation temperature with drug (BSP-loaded formulation).

hydrophilicity compared to P407. This characteristic disrupts efficient micellar packing by diluting the hydrophobic interactions necessary for gel formation. Concurrently, increasing concentration of HA contributes to the overall viscosity of the system. Due to its high molecular weight and extended coil structure in aqueous environments, it promotes polymer chain entanglements, which hinder the mobility of poloxamer micelles and delay their aggregation into a structured gel network. This combined effect of P188 and HA results in prolonged gelation times and elevated gelation temperatures (Cook et al. 2021).

### Drug–excipient compatibility

The FTIR scan performed for BSP revealed characteristic peaks at  $3412\text{ cm}^{-1}$  representing the O–H stretching band, C–H stretching at  $2981$  and  $2937\text{ cm}^{-1}$ , strong

peaks corresponding to C=O (carbonyl group) stretching, bending vibrations of  $\text{CH}_2$  at  $1452$  and  $1392\text{ cm}^{-1}$ , and stretching modes from phosphate ester group C–O and P=O at  $1246$ – $1099\text{ cm}^{-1}$ . The spectrum of P407 showed characteristic peaks at  $3477\text{ cm}^{-1}$  for O–H stretching,  $2877$ – $2692\text{ cm}^{-1}$  for C–H stretching,  $\text{CH}_2$  bending, and ether C–O–C vibrations at  $1469$ – $1242\text{ cm}^{-1}$ . The FTIR spectrum of P188 is very similar to P407 but shows more intense ether bands, which is consistent with previous studies (Desai et al. 2022). The HA FTIR spectrum represented broad O–H stretching due to the hydroxyl group, aliphatic C–H stretching at  $2922$  and  $2870\text{ cm}^{-1}$ , C=O stretching of the carboxyl group at  $1735$  and  $1651\text{ cm}^{-1}$ , and carboxyl ( $\text{COO}^-$ ) symmetric and asymmetric stretching at  $1562$  and  $1454\text{ cm}^{-1}$ . The spectrum for the PM retained the characteristic O–H stretching of BSP at  $3412\text{ cm}^{-1}$  but appeared broader and slightly shifted, likely due to hydrogen bonding

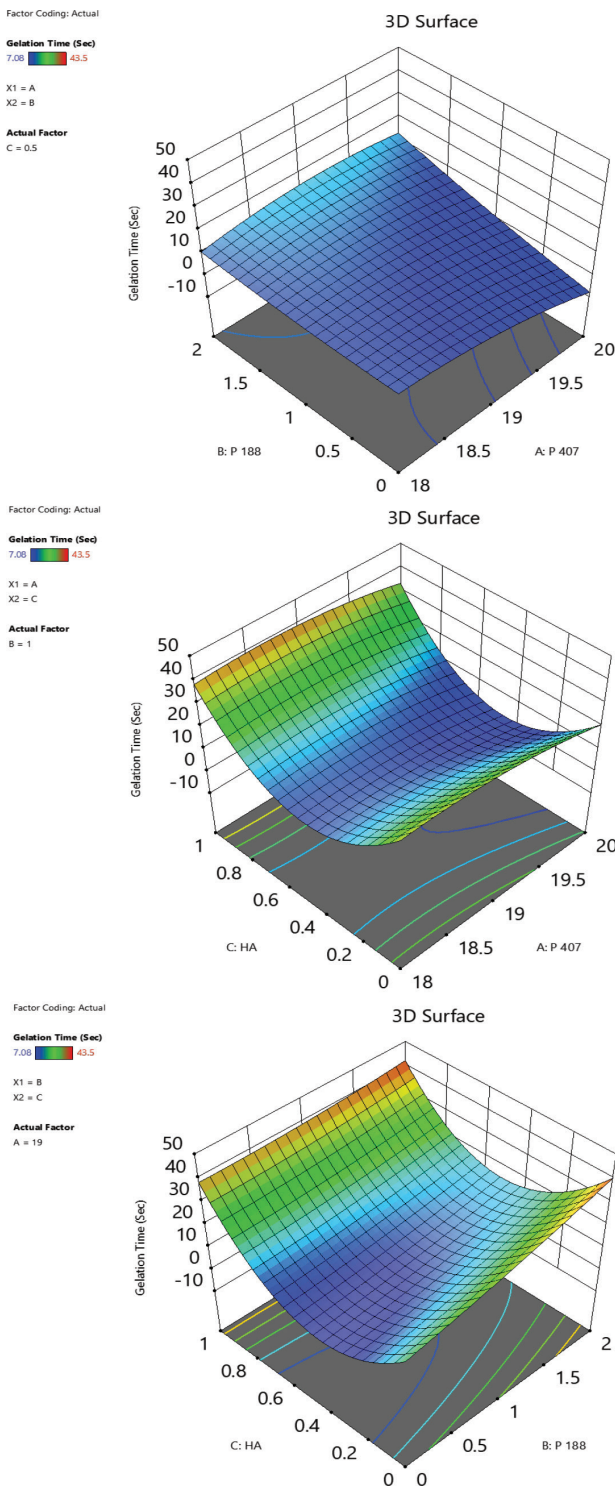


**Figure 6.** 3D response surface plots illustrating the effect of formulation variables on gelation time ( $Y_3$ ).

with excipients. No new peaks were observed, which suggests there are no chemical interactions between the materials used (Fig. 7).

### Optimization of BSP-loaded IG formulations by numerical method

Numerical optimization was employed using the desirability function approach to achieve optimal formula-

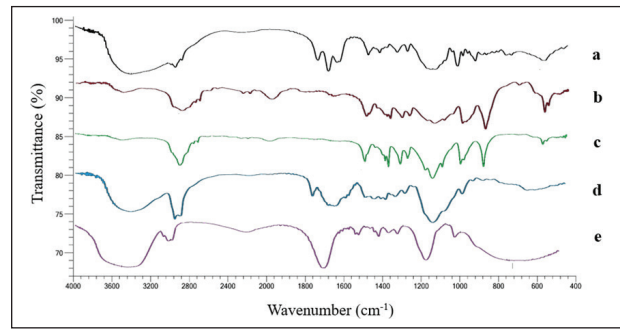


**Figure 7.** FTIR spectrum: a. BSP; b. P407; c. P188; d. HA, e. PM.

tion parameters. Seven of the suggested formulas with a desirability factor of 1 were evaluated for their gelation temperature and time; their actual and predicted values are presented in Table 4. The experimentally measured (actual) values were in close agreement with the predicted values, verifying the effectiveness of the desirability approach.

## Characterization of optimized formulas

### Appearance and pH evaluation

All prepared optimized formulas appeared clear, transparent, and homogeneous. The pH values of the optimized formulas ranged from  $7.0 \pm 0.05$  to  $7.2 \pm 0.05$  (Table 5). All formulations showed acceptable pH values (7.0–7.2) that would not irritate the oral cavity upon application (Raheema and Kassab 2022).

### Gelling capacity

All the optimized formulas, upon contact with the buffer medium, underwent a phase transition (sol-to-gel) due to the presence of thermosensitive polymers. The gelling capacity results demonstrated that as the concentrations of P407 and HA increased from 18.046% to 20% and 0.278% to 0.5%, respectively, the time needed for the formula to dissolve also increased—from  $1.25 \pm 0.2$  h (F1) to  $2.33 \pm 0.24$  h (F7), as shown in Table 5 (Alabdly and Kassab 2023).

### Viscosity determination

The viscosity measurements of all optimized formulations exhibited pseudoplastic shear-thinning behavior both before and after gelation. The viscosity values of formulations decreased as the applied shear rate increased (Fig. 8). At room temperature, all seven formulas showed viscosities lower than 1000 mPa·s, which was necessary to allow fluid release from the spray (Bastos et al. 2024). The change in viscosity upon raising the temperature indicates the thermosensitive nature of the prepared IG. An increase in viscosity was observed with rising HA concentrations, which may be attributed to polymer chain entanglement. Similarly, a higher poloxamer concentration (as in F7) also contributed to the increased viscosity (Alkufi and Kassab 2019).

**Table 4.** Optimized formulas: predicted vs. actual values.

| Formula | P407%  | P188% | HA%   | Gelation temperature (C°) |            | Gelation time (s) |              |
|---------|--------|-------|-------|---------------------------|------------|-------------------|--------------|
|         |        |       |       | Predicted                 | Actual     | Predicted         | Actual       |
| F1      | 18.046 | 1.441 | 0.278 | 33.3                      | 33.1 ± 0.2 | 13.8              | 13.70 ± 2.16 |
| F2      | 18.024 | 1.354 | 0.703 | 34.4                      | 33.7 ± 1.5 | 14.6              | 13.32 ± 2.7  |
| F3      | 19.016 | 1.666 | 0.337 | 33.4                      | 34.0 ± 0.9 | 14.8              | 15.43 ± 2.5  |
| F4      | 19.230 | 1.668 | 0.608 | 33.7                      | 33.3 ± 0.7 | 14.3              | 14.79 ± 1.87 |
| F5      | 19.750 | 1.950 | 0.375 | 33.3                      | 33.9 ± 0.9 | 14.9              | 14.53 ± 3.65 |
| F6      | 19.861 | 1.883 | 0.614 | 33.2                      | 33.1 ± 0.4 | 14.4              | 13.43 ± 1.58 |
| F7      | 20.000 | 2.000 | 0.500 | 33.1                      | 33.6 ± 0.2 | 13.2              | 11.24 ± 2.12 |

**Table 5.** Evaluation of optimized formulations.

| Formula | Appearance | pH         | Gelation capacity (h) |
|---------|------------|------------|-----------------------|
| F1      | Clear      | 7.0 ± 0.05 | 1.25 ± 0.2            |
| F2      | Clear      | 7.1 ± 0.05 | 1.42 ± 0.12           |
| F3      | Clear      | 7.1 ± 0.09 | 1.50 ± 0.2            |
| F4      | Clear      | 7.2 ± 0.08 | 2.24 ± 0.2            |
| F5      | Clear      | 7.0 ± 0.13 | 1.92 ± 0.12           |
| F6      | Clear      | 7.1 ± 0.09 | 2.17 ± 0.12           |
| F7      | Clear      | 7.2 ± 0.05 | 2.33 ± 0.24           |

### Texture analysis profile of optimized formulas

The TPA was performed to evaluate the mechanical properties of the optimized oral gel formulations. The analysis focused on key parameters: hardness, compressibility, adhesiveness, and cohesiveness. The results of TPA demonstrate a clear effect of P407 and P188 concentrations on gel texture parameters (Table 6). Increasing the P407 concentration was associated with higher values for hardness, compressibility, and adhesiveness, indicating firmer gel formation and improved mucoadhesion. Formula F1, with the lowest polymer concentrations, showed the lowest values in all parameters, suggesting a weaker and less structured gel. Cohesiveness values ranged from 0.86 to 1.49, with the highest value observed in formulation F7, indicating increased bonding within the gel matrix, as previously indicated by its highest viscosity. In particular, Formula F4 exhibited the highest hardness (37.72 g), compressibility (42.09 g·s), and adhesiveness (33.92 g·s), indicating a dense and cohesive gel structure, followed by Formula F6, which also yielded values superior to those of the remaining formulas. These results highlight the importance of poly-

**Table 6.** Texture profile analysis results of optimized formulas.

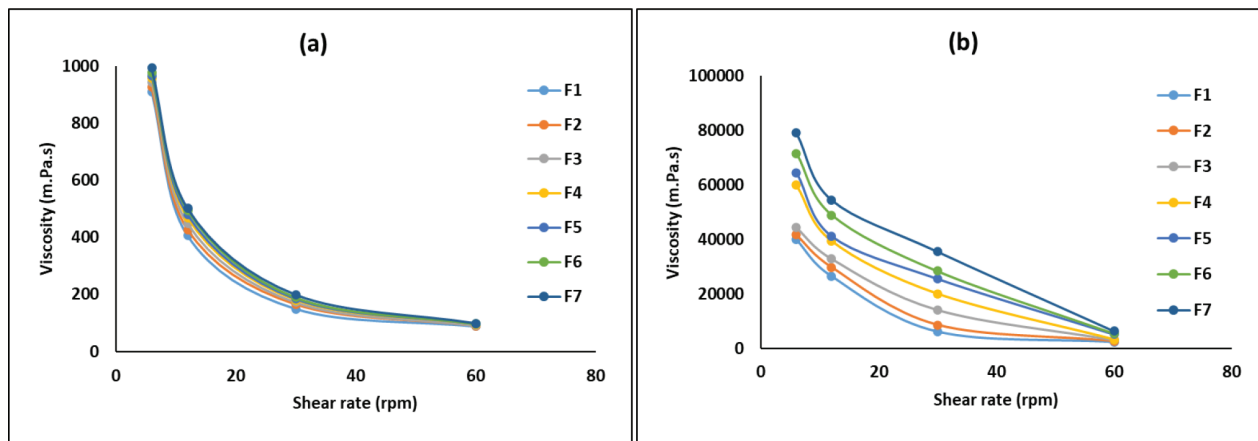
| Formula | Hardness (g) | Compressibility (g·s) | Adhesiveness (g·s) | Cohesiveness (dimensionless) |
|---------|--------------|-----------------------|--------------------|------------------------------|
| F1      | 5.08         | 0.24                  | 0.21               | 0.86                         |
| F2      | 7.42         | 8.96                  | 0.22               | 1.10                         |
| F3      | 11.14        | 11.17                 | 7.99               | 0.97                         |
| F4      | 37.72        | 42.09                 | 33.92              | 1.09                         |
| F5      | 16.90        | 21.21                 | 15.14              | 1.02                         |
| F6      | 31.91        | 52.35                 | 49.43              | 1.27                         |
| F7      | 24.21        | 38.48                 | 38.09              | 1.49                         |

mer composition in tailoring the mechanical behavior of topical oral gels to achieve appropriate structure retention and patient comfort (Desai et al. 2022).

Meanwhile, the TPA results for optimized formulas in their liquid state at room temperature showed relatively low mechanical strength, as expected for the sol phase, indicating poor structural integrity in the sol phase, which is desirable for ease of spraying before sol-gel transition at physiological temperatures (Adisanoğlu and Özgüney 2024).

### Mucoadhesion study

The mucoadhesion properties of optimized formulations were evaluated by measuring both  $F_{adh}$  (force of detachment) and  $W_{adh}$  (work of adhesion), as shown in Table 7. Among all formulations, F4, F6, and F7 may be considered to have good mucoadhesion properties, where F6 exhibited the highest  $F_{adh}$  of 92.97 g and  $W_{adh}$  value of -298.41 g·s, demonstrating excellent mucoadhesion strength. In addition, F4 also demonstrated strong mucoadhesion, with  $F_{adh}$  67.68 g and  $W_{adh}$  -297.02 g·s. Formula F7 also exhibited relatively good mucoadhesion properties, with  $F_{adh}$  92.97 g and  $W_{adh}$  -293.72 g·s, compared

**Figure 8.** Viscosity of optimized formulas measured at a. Room temperature ( $25 \pm 1$  °C) before gelation and b. Physiological temperature ( $37 \pm 1$  °C) after gelation.

**Table 7.** Mucoadhesion properties of optimized formulas.

| Formula ID             | F1      | F2      | F3      | F4      | F5      | F6      | F7      |
|------------------------|---------|---------|---------|---------|---------|---------|---------|
| F <sub>adh</sub> (g)   | 11.53   | 24.13   | 18.64   | 67.68   | 25.07   | 92.97   | 59.2    |
| W <sub>adh</sub> (g.s) | -232.94 | -282.69 | -252.33 | -297.02 | -287.41 | -298.41 | -293.72 |

to the remaining formulas. These high values can be attributed to the increased concentrations of polymers, which contribute to improved gel consistency and stronger interaction with the mucin tablet. In contrast, F1 exhibited the lowest mucoadhesion performance, confirming that lower polymer and HA concentrations result in poor adhesion properties (Karaküçük and Tort 2021). A statistically significant effect was observed for HA on the work of adhesion ( $p = 0.023$ ), indicating that increasing HA concentration positively influences the extent of mucoadhesion.

## Spray performance evaluation

### Spray angle

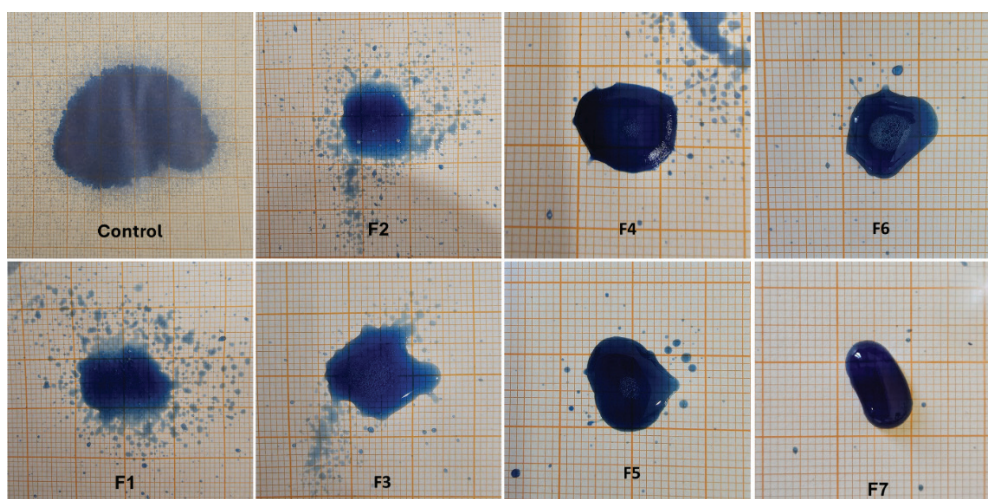
The spray angle is a critical factor in evaluating the performance of oral topical gel sprays, as it directly reflects the formula coverage area upon spray application. The control solution, containing the drug in DW, exhibited the widest spray angle, reaching  $76.1 \pm 0.58^\circ$  at a nozzle height of 3 cm, demonstrating broad dispersion and minimal flow resistance due to the low viscosity of DW compared with gel-forming polymers. In contrast, formulations containing thermosensitive polymers and HA exhibited a progressively lower spray angle. For example, F7, which included the highest concentrations of P407 (20%), P188 (2%), and HA (0.5%), exhibited the narrowest spray angle of  $22.6 \pm 1.63^\circ$  at a height of 3 cm (Table 8), which is expected due to its high viscosity. F6 exhibited a slightly bigger spray angle at both nozzle heights (approximately  $33.4^\circ$ ), indicating a narrow and somewhat asymmetric spray plume. Meanwhile, F4 exhibited a spray angle of  $43.6 \pm 0.62^\circ$  at 3 cm and  $42.6 \pm 1.39^\circ$  at 6 cm. The overall results suggest that increasing the polymer content resulted in a gradual decrease in the spray angle, attributed to the higher viscosity that restricts the atomization of the spray (Ranade et al. 2017).

**Table 8.** Spray plume parameters.

| Formula | Nozzle height (cm) | Dmax (cm)      | Dmin (cm)      | Ovality ratio  | Spray angle ( $^\circ$ ) |
|---------|--------------------|----------------|----------------|----------------|--------------------------|
| Control | 3                  | $4.7 \pm 0.58$ | $4.5 \pm 1.64$ | $1.1 \pm 0.03$ | $76.1 \pm 0.58$          |
|         | 6                  | $8.8 \pm 0.79$ | $8.1 \pm 0.23$ | $1.1 \pm 0.03$ | $72.7 \pm 0.79$          |
| F1      | 3                  | $3.2 \pm 1.16$ | $3.2 \pm 1.30$ | $1 \pm 0.0$    | $56.1 \pm 1.16$          |
|         | 6                  | $5.3 \pm 1.96$ | $4.9 \pm 0.10$ | $1.1 \pm 0.07$ | $55.8 \pm 1.96$          |
| F2      | 3                  | $3 \pm 0.76$   | $2.8 \pm 0.60$ | $1.1 \pm 0.04$ | $53.1 \pm 0.76$          |
|         | 6                  | $5.1 \pm 2.38$ | $4.1 \pm 1.07$ | $1.3 \pm 0.28$ | $54 \pm 2.38$            |
| F3      | 3                  | $2.8 \pm 1.58$ | $2.7 \pm 0.97$ | $1 \pm 0.05$   | $50 \pm 1.58$            |
|         | 6                  | $4.6 \pm 1.61$ | $3.9 \pm 0.57$ | $1.2 \pm 0.14$ | $49.4 \pm 1.61$          |
| F4      | 3                  | $2.4 \pm 0.62$ | $2.2 \pm 0.12$ | $1.1 \pm 0.06$ | $43.6 \pm 0.62$          |
|         | 6                  | $3.9 \pm 1.39$ | $3.8 \pm 0.14$ | $1 \pm 0.03$   | $42.6 \pm 1.39$          |
| F5      | 3                  | $2 \pm 1.92$   | $1.1 \pm 0.48$ | $2 \pm 1.07$   | $36.9 \pm 1.92$          |
|         | 6                  | $3.3 \pm 0.37$ | $2.6 \pm 0.37$ | $1.3 \pm 0.22$ | $36.5 \pm 0.37$          |
| F6      | 3                  | $1.8 \pm 1.98$ | $1.1 \pm 0.44$ | $1.6 \pm 0.03$ | $33.4 \pm 1.98$          |
|         | 6                  | $3 \pm 0.35$   | $2.1 \pm 0.87$ | $1.6 \pm 0.29$ | $33.4 \pm 0.35$          |
| F7      | 3                  | $1.2 \pm 1.63$ | $0.9 \pm 0.71$ | $1.5 \pm 0.17$ | $22.6 \pm 1.63$          |
|         | 6                  | $2 \pm 1.51$   | $1.3 \pm 0.84$ | $1.7 \pm 0.33$ | $22.5 \pm 1.51$          |

### Spray pattern and ovality ratio

The spray plume's geometrical characteristics were evaluated by measuring Dmax, Dmin, and the ovality ratio at two nozzle heights (Table 8). The control formula exhibited the largest spray diameters, with Dmax values of  $4.7 \pm 0.58$  cm and  $8.8 \pm 0.79$  cm at heights of 3 cm and 6 cm, respectively. It also displayed nearly circular spray patterns with an ovality ratio of  $1.1 \pm 0.03$ . As the polymer concentrations increased from formulation F1 to F7, both Dmax and Dmin gradually decreased, indicating that increasing the viscosity of the formulations reduced the spread of the spray plume. While formulations (F1–F4) relatively maintained near-circular spray patterns with ovality ratios of  $1 \pm 0.0$  to  $1.2 \pm 0.14$  (Fig. 9), higher-viscosity formulations (F5–F7) exhibited significantly higher ovality ratios. For instance, in F7, the spray pattern became narrow and distorted (ovality ratio  $1.5 \pm 0.17$  at 3 cm height), possibly due to insufficient atomization associated with the high viscosity. The results suggest that excessive viscosity may hinder spray efficacy and affect dose uniformity (Hegde et al. 2025). The spray angle and the height of the nozzle above the target surface primarily influence the spray pattern. A wider spray angle results in

**Figure 9.** Spray plume pattern of optimized formulas sprayed from a vertical distance of 3 cm.

a broader coverage area, enabling the spray to reach a larger surface area in a single application (Swami et al. 2016).

Notably, an increase in nozzle height was associated with a slight reduction or stabilization in spray angle and a concurrent rise in ovality ratio. These findings suggest that higher nozzle heights can distort spray geometry, likely due to increased gravitational and air drift effects, which reduce spray dispersion and elongate the spray plume (Kumar and Dash 2018). Results demonstrated that a 3 cm height consistently yielded more favorable spray angles and lower ovality ratios, indicating better plume symmetry and dispersion. Based on the TPA, mucoadhesion results, and spray plume characteristics, F4 and F6 were selected for further spray evaluations in comparison to the control spray.

### Automated spray actuation evaluation

Actuation force and maximum force for actuation measurements showed a gradual increase in resistance with increasing spray formulation viscosity (Table 9). The control spray exhibited the lowest actuation force at 1.3 kg.f and a maximum force of 1.4 kg.f, indicating the lowest mechanical resistance. Both formulas (F4 and F6) tested remained within the FDA actuation force limits of < 5.8 kg.f for adults and < 3.4 kg.f for children. The results indicate that the tested formulations are mechanically acceptable for patient use (Bastos et al. 2024).

**Table 9.** Automated spray measurements.

| Formula ID             | Control    | F4         | F6         |
|------------------------|------------|------------|------------|
| Actuation Force (kg.f) | 1.3 ± 0.02 | 1.5 ± 0.01 | 1.9 ± 0.05 |
| Maximum Force (kg.f)   | 1.4 ± 0.01 | 1.6 ± 0.00 | 2.5 ± 0.07 |

### Spray delivery profile (delivered plume uniformity)

The spray plume delivery profiles of selected formulas (F4 and F6) and the control spray are shown in Fig. 10. The results indicate low variability in the in-use actuation of all tested sprays, as the individual plume weight values fall within the FDA acceptance criteria, ± 15% of the target weight of each spray formulation, and the mean is within ± 10% (FDA 2002) (Table 10). The number of priming actuations increases as the viscosity of the formulation increases; for the control spray, there were five plumes. Meanwhile, F4 and F6 needed eight and ten plumes, respectively, before reaching their consistent plume weight. In addition, the amount of formula that remained in the sprays after exhaustion (mass lost) was also highly influenced by the viscosity of the formulations.

**Table 10.** Spray delivery profile elements.

| Formula ID | Formulation weight (g) | Plume target weight (mg) | Priming shots number | In-use actuations numbers | Mass lost (g) |
|------------|------------------------|--------------------------|----------------------|---------------------------|---------------|
| Control    | 15.1                   | 232 ± 8.72               | 5                    | 88                        | 0.2           |
| F4         | 15.1                   | 145 ± 2.42               | 8                    | 100                       | 0.3           |
| F6         | 15.1                   | 136 ± 3.19               | 10                   | 104                       | 0.6           |

### Spray drug content

The drug content per spray actuation was  $99.5 \pm 0.67\%$  and  $99 \pm 1.51\%$  for F4 and F6, respectively. Both formulations were within the limits of 85% to 115% (Pawar et al. 2021).

### In vitro release study kinetics

The in vitro release profiles of F4, F6, and the control spray were compared using a Franz cell over 120 minutes. The control spray solution showed an immediate release burst, reaching  $99.5 \pm 0.19\%$  within 20 minutes. Meanwhile, F4 and F6 demonstrated a gradual and relatively more delayed drug release. The F4 formulation exhibited a relatively faster drug release, with  $97.9 \pm 1.46\%$ , compared to F6, which resulted in  $90.8 \pm 2.87\%$  after 105 minutes (Fig. 11). The similarity factors ( $f_2$ ) of the control spray and selected formulations (F4 and F6) were 31.43 and 25.71, respectively, indicating that the F4 and F6 formulations had significantly slower drug release profiles than the control, likely due to the presence of polymers (Alkufi and Kassab 2019). According to the above results, formula F4 was selected for further irritation study due to its balanced performance across key parameters, including a gelation temperature close to physiological conditions, acceptable spray characteristics that showed uniform coverage with an appropriate angle and plume, strong mucoadhesion, suitable viscosity, and a superior drug release profile. These attributes made it the most promising among the tested formulations.

### Histological irritation study

The macroscopic examination of the oral cavity mucosa was evaluated visually before and after application of the F4 formula. No adverse reaction of any form was detected after 24 h of application. Furthermore, the histopathological figures of the buccal mucosa in both control and treatment groups showed normal lining epithelial cells, normal subepithelial collagen fibers, and skeletal muscle fibers. The magnification power revealed normal cytoarchitecture of cells and blood vessels. The histopathological figures of the glossal mucosa in both control and treatment groups also revealed normal lingual papillae, normal lining epithelial cells, normal subepithelial collagen fibers, and skeletal muscle fibers (Fig. 12: microscopic slide image with 100x magnification).

## Conclusion

This study successfully developed a novel mucoadhesive in situ gel-forming oral spray containing beta-methasone sodium phosphate, utilizing P407 and P188 as gel-forming polymers and hyaluronic acid for its mucoadhesive and healing properties. The optimized formulation exhibited desirable gelation temperatures, gelation times, spray profile, mucoadhesion, and mechanical strength suitable for oral mucosal applications.

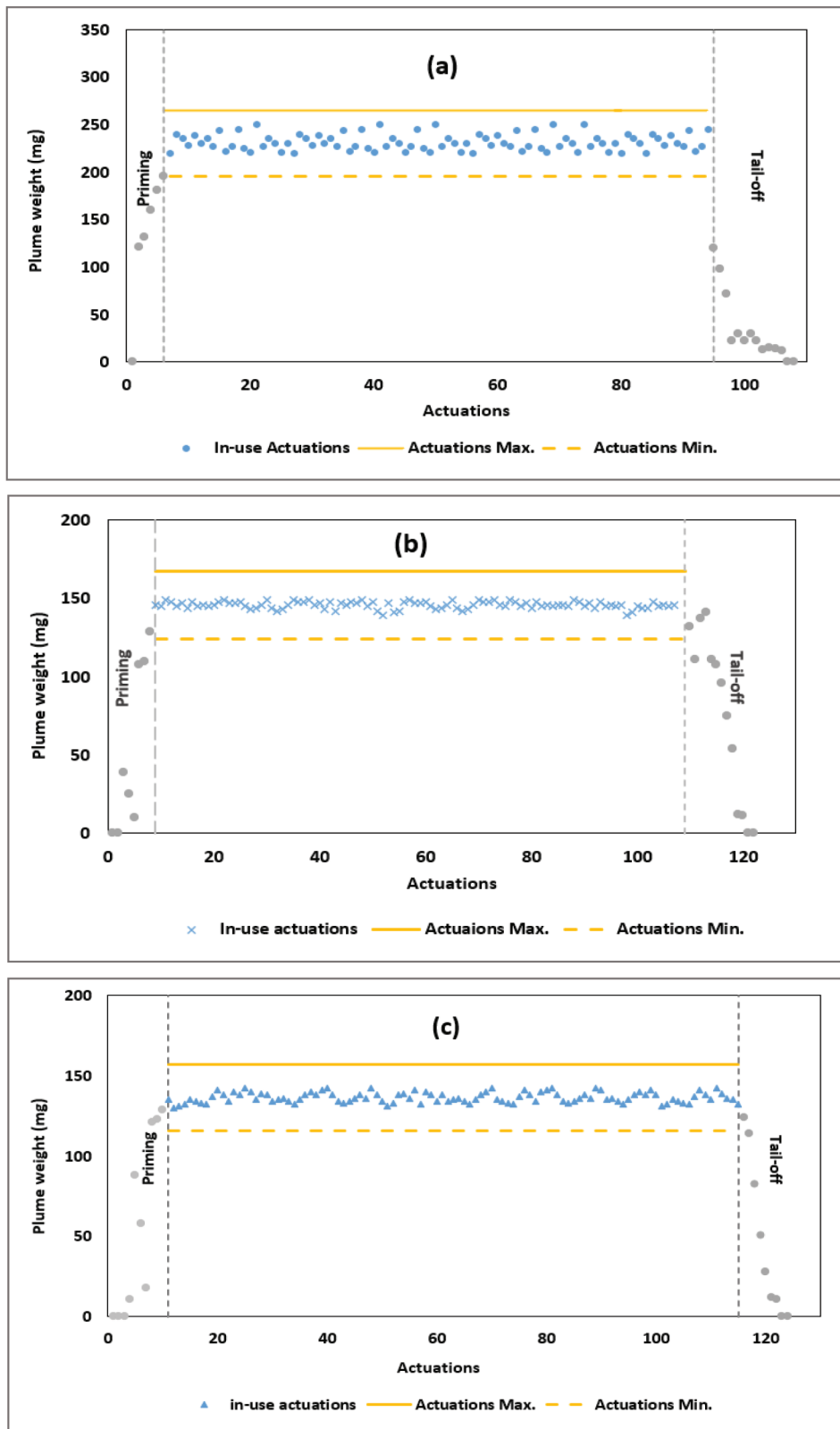


**Figure 10.** Spray delivery profile with maximum and minimum limits of acceptance criteria for **a.** Control spray, **b.** F4 spray, and **c.** F6 spray. The yellow lines represent the minimum and maximum limits for the accepted criteria ( $\pm 15\%$ ) of the target actuation weight.

This novel delivery system overcomes key limitations of conventional ulcer treatments by forming a gel upon contact with body temperature and adhering to the mucosal surface. The spray ensures prolonged drug

residence time and improves patient comfort through ease of application, making it a promising therapeutic strategy for managing oral ulcers and warranting further clinical investigation. The evaluation was restricted

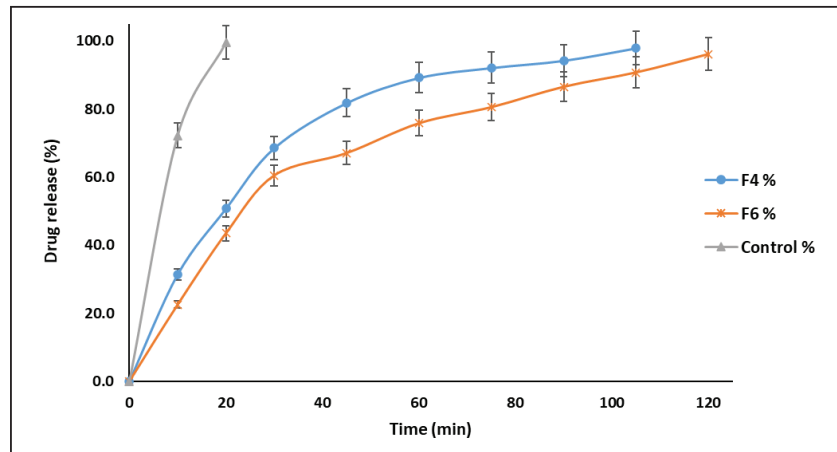


**Figure 11.** Release profile of control spray, F4, and F6 formulations at pH 6.8 and 37 °C (mean  $\pm$  SD, n = 3).

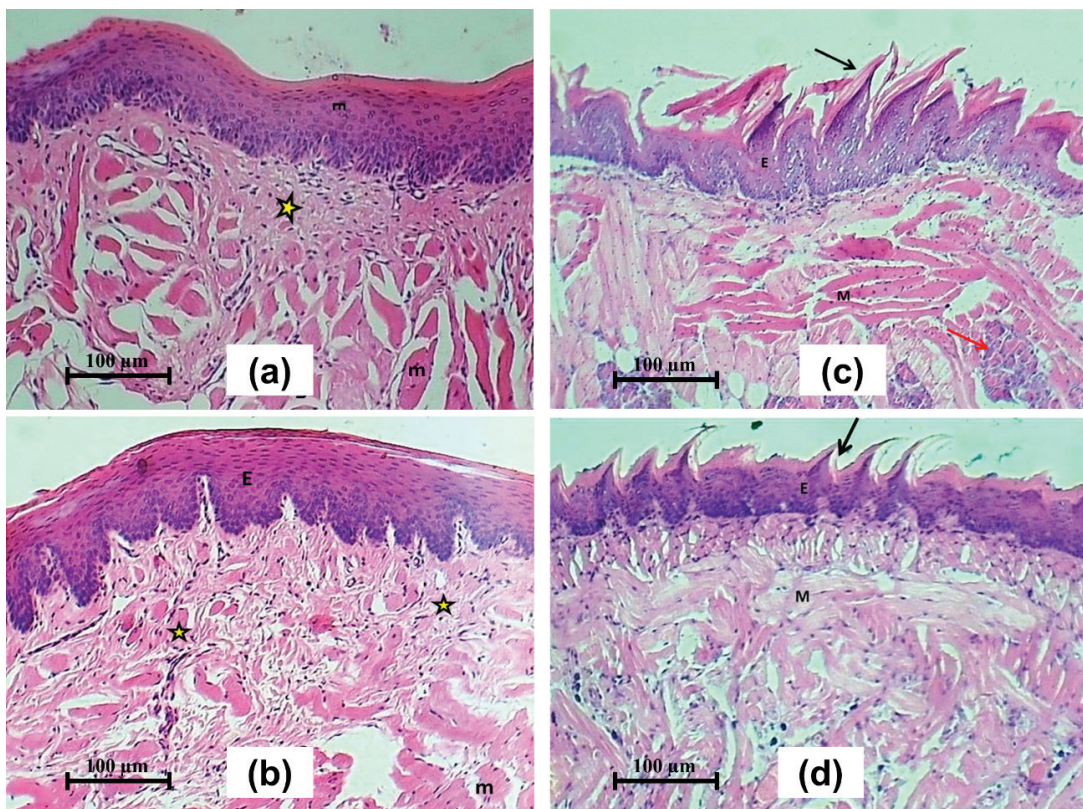


**Figure 12.** a. Section of buccal mucosa (control) shows normal epithelial cells (E) and normal skeletal muscle fibers (m); b. Section of buccal mucosa (treatment group); c. Section of the tongue (control group) shows normal lingual papilla (black arrow) and glossal salivary glands (red arrows); d. Section of the tongue (treatment group) shows normal lingual papilla (arrow).

to in vitro and preclinical mucosal irritation; thus, in vivo validation in animal or clinical models is necessary to confirm therapeutic effectiveness and patient-taste acceptability. Additionally, long-term stability under various storage conditions and the effects of repeated application warrant further investigation.

## Competing interests

The authors have declared that no competing interests exist.

## Acknowledgments

The authors sincerely thank the Department of Pharmaceutics at the College of Pharmacy, University of Baghdad, for their continued support.

## Additional information

### Conflict of interest

The authors have declared that no competing interests exist.

## Ethical statements

The authors declared that no clinical trials were used in the present study.

The authors declared that no experiments on humans or human tissues were performed for the present study.

The authors declared that no informed consent was obtained from the humans, donors or donors' representatives participating in the study.

Experiments on animals: REC032433R.

The authors declared that no commercially available immortalised human and animal cell lines were used in the present study.

## Use of AI

No use of AI was reported.

## Funding

No funding was reported.

## Author contributions

Mawadda B. Al-Juboori: Conceptualization, Formal analysis, Methodology, Writing. Eman B. H. Al-Khedairy: Supervision, Validation, Writing – review & editing.

## Author ORCIDs

Mawadda B. Al-Juboori  <https://orcid.org/0009-0004-6127-4045>

## Data availability

All of the data that support the findings of this study are available in the main text or Supplementary Information.

## References

- Al-Sawaf OFB, Jalal F (2023) Novel probe sonication method for the preparation of meloxicam bilosomes for transdermal delivery: part one. *Journal of Research in Medical and Dental Science*, 11. <https://www.jrmds.in>
- Alkufi HK, Kassab HJ (2019) Formulation and evaluation of sustained release sumatriptan mucoadhesive intranasal in-situ gel. *Iraqi Journal of Pharmaceutical Sciences* 28(2): 95–104. <https://doi.org/10.31351/vol28iss2pp95-104>
- Alptuğ K, Tort S (2021) Formulation, optimization, and in-vitro evaluation of hyaluronic acid buccal films containing benzydamine hydrochloride. *Journal of Duzce University Health Sciences Institute* 11(3): 325–330. <https://doi.org/10.33631/duzcesbed.833024>
- Ammar A, Kassab HJ (2023) Formulation variables effect on gelation temperature of nefopam hydrochloride intranasal in situ gel (conference paper). *Iraqi Journal of Pharmaceutical Sciences* 31: 32–44. <https://doi.org/10.31351/vol31issSuppl.pp32-44>
- Atoosh Ilaf J and Mowafaq M Ghareeb (2024) Optimizing mucoadhesive film-forming spray for efficient oral delivery of fluconazole in candidiasis treatment. *Cureus* 16(9): e70359. <https://doi.org/10.7759/cureus.70359>
- Bakhrushina EO, Khodenok AI, Pyzhov VS, Solomatina PG, Demina NB, Korochkina TV, Krasnyuk II (2023) Study of the effect of active pharmaceutical ingredients of various classes of bcs on the parameters of thermosensitive systems based on poloxamers. *Saudi Pharmaceutical Journal* 31(10): 101780. <https://doi.org/10.1016/j.jsps.2023.101780>
- British Pharmacopoeia Commission British Pharmacopoeia (2022) Tenth. Vol. 5. London: The Stationery Office (MHRA). <http://www.pharmacopoeia.com>
- Cook MT, Haddow P, Kirton SB, McAuley WJ (2021) Polymers exhibiting lower critical solution temperatures as a route to thermoreversible gels for healthcare. *Advanced Functional Materials* 31(8): 2008123. <https://doi.org/10.1002/adfm.202008123>
- da Silva B, Jéssica SF, Reis A, Cook M, Bruschi M (2018) Assessing mucoadhesion in polymer gels: the effect of method type and instrument variables. *Polymers* 10(3): 254. <https://doi.org/10.3390/polym10030254>
- Dedhiya M, Economou JJ (2002) Fluticasone Suspension Formulation, Spray Pattern Method, and Nasal Spray Apparatus. US 2002O132803A1, issued September 19, 2002.
- Doughty DV, Vibbert C, Kewalramani A, Bollinger ME, Dalby RN (2011) automated actuation of nasal spray products: determination and comparison of adult and pediatric settings. *Drug Development and Industrial Pharmacy* 37(3): 359–366. <https://doi.org/10.3109/03639045.2010.520321>
- FDA [U.S. Food and Drug Administration] (2002) Guidance for Industry Nasal Spray and Inhalation Solution, Suspension, and Spray Drug Products—Chemistry, Manufacturing, and Controls Documentation. <http://www.fda.gov/cder/guidance/index.htm>
- Francisca B, Tabanez A, Aquino M, Nunes A, Simões S (2024) Oromucosal spray products – viscosity impact on spray performance evaluation. *Journal of Drug Delivery Science and Technology* 94: 105480. <https://doi.org/10.1016/j.jddst.2024.105480>
- Hamzah L Mohammed and Hanan Jalal Kassab (2024) Formulation and development of frovatriptan succinate in situ gel for nasal drug delivery: in vitro and ex vivo evaluation. *Pakistan Journal of Pharmaceutical Sciences* 37(3): 511–21. <https://doi.org/doi.org/10.36721/PJPS.2024.37.3>
- Harekrishna GN, Husukale PS (2023) Development and evaluation of in situ gel formation for treatment of mouth ulcer. *Turkish Journal of Pharmaceutical Sciences* 20(3): 185–197. <https://doi.org/10.4274/tjps.galenos.2022.25968>
- Hsieh H-Y, Lin W-Y, Lee AL, Li Y-C, Chen Y J, Chen K-C, Young T-H (2020) Hyaluronic acid on the urokinase sustained release with a hydrogel system composed of poloxamer 407: HA/P407 hydrogel system for drug delivery. *PLoS ONE* 15(3): e0227784. <https://doi.org/10.1371/journal.pone.0227784>
- Inchara R, Uma Maheshwari TN (2020) In situ gel treatment for oral mucosal lesions: a systematic review. *Journal of International Oral Health* 12(6): 499. [https://doi.org/10.4103/JIOH.JIOH\\_257\\_20](https://doi.org/10.4103/JIOH.JIOH_257_20)
- Jackson R, Fiegel J, Brogden NK (2022) Effect of salt form on gelation and drug delivery properties of diclofenac-loaded poloxamer gels for delivery to impaired skin. *Pharmaceutical Research* 39(10): 2515–2527. <https://doi.org/10.1007/s11095-022-03356-1>
- Jaenjira A, Samee W, Tadtong S, Mangmool S, Okonogi S, Toolmal N, Chittasupho C (2025) Development, optimization, and stability study of a yataprasen film-forming spray for musculoskeletal pain management. *Gels* 11(1): 64. <https://doi.org/10.3390/gels11010064>

- Jan M, Komersová A, Kubová K, Matzick K, Skalická B (2021) A critical overview of FDA and EMA Statistical methods to compare in vitro drug dissolution profiles of pharmaceutical products. *Pharmaceutics* 13(10): 1703. <https://doi.org/10.3390/pharmaceutics13101703>
- Khudhaier OK, Thomas LM (2025) Formulation and evaluation of melizine hydrochloride cyclodextrin-based mucoadhesive thermosensitive in-situ gel. *Iraqi Journal of Pharmaceutical Sciences* 34(1): 2025. <https://doi.org/10.31351/vol34iss1pp108-121>
- Kumar A, Dash BS (2018) Effect of nozzle type, pressure and height on spray distribution pattern and droplet characteristic. *CABI Digital Library* 823–28.
- Lan WY, Pandey M, Choudhury H, Lim WM, Bhattamisra SK, Gorain B (2021) Development of in-situ spray for local delivery of antibacterial drug for hidradenitis suppurativa: investigation of alternative formulation. *Polymers* 13(16): 2770. <https://doi.org/10.3390/polym13162770>
- Laura M, De Stefano D, De Falco F, Carnuccio R, Maiuri MC, De Rosa G (2014) Effect of hyaluronic acid on the thermogelation and biocompatibility of its blends with methyl cellulose. *Carbohydrate Polymers* 112: 480–485. <https://doi.org/10.1016/j.carbpol.2014.06.020>
- Lee JH, Jung JY, Bang D (2008) The efficacy of topical 0.2% hyaluronic acid gel on recurrent oral ulcers: comparison between recurrent aphthous ulcers and the oral ulcers of behçet's disease. *Journal of the European Academy of Dermatology and Venereology* 22(5): 590–595. <https://doi.org/10.1111/j.1468-3083.2007.02564.x>
- Li T, Bao Q, Shen J, Lalla RV, Burgess DJ (2020a) Mucoadhesive in situ forming gel for oral mucositis pain control. *International Journal of Pharmaceutics* 580: 119238. <https://doi.org/10.1016/j.ijpharm.2020.119238>
- Li T, Bao Q, Shen J, Lalla RV, Burgess DJ (2020b) Mucoadhesive in situ forming gel for oral mucositis pain control. *International Journal of Pharmaceutics* 580: 119238. <https://doi.org/10.1016/j.ijpharm.2020.119238>
- Manjunath HA, Syed A, Karwa P (2025) Spray angle measurement in pharmaceutical sprays: correct methodology and common pitfalls. *Journal of Pharmaceutical Innovation* 20(1): 8. <https://doi.org/10.1007/s12247-024-09919-6>
- Martins FI, Camila FFP, Camila dos Santos M, Saviano AM, Lourenço FR (2018) Design of experiments (doe) applied to pharmaceutical and analytical quality by design (QbD). *Brazilian Journal of Pharmaceutical Sciences* 54(spe). <https://doi.org/10.1590/s2175-97902018000001006>
- Pawar Neelam, Anoop Parmar, Kavita Bahmani, DN Mishra, Renu Malik, Neha Minocha, Pawan Jalwal, and Rahul Pawar (2021) Formulation, optimization and evaluation of non-aerosol topical spray of lidocaine for pain management. *International Journal of Pharmaceutical Investigation* 11(4): 414–419. <https://doi.org/10.5530/ijpi.2021.4.74>
- Pınar A, Özgüney I (2024) Development and characterization of thermosensitive and bioadhesive ophthalmic formulations containing flurbiprofen solid dispersions. *Gels* 10(4): 267. <https://doi.org/10.3390/gels10040267>
- Raheema DA, Kassab HJ (2022) Preparation and in-vitro evaluation of secnidazole as periodontal in-situ gel for treatment of periodontal disease. *Iraqi Journal of Pharmaceutical Sciences* 31(2): 50–61. <https://doi.org/10.31351/vol31iss2pp50-61>
- Rudralingam M, Randall C, Mighell AJ (2017) The use of topical steroid preparations in oral medicine in the UK. *British Dental Journal* 223(9): 633–638. <https://doi.org/10.1038/sj.bdj.2017.880>
- Salfuqi N, Yulia R, Irmayanti EN, Sunarti TC (2019) The optimization of gel preparations using the active compounds of arabica coffee ground nanoparticles. *Scientia Pharmaceutica* 87(4): 32. <https://doi.org/10.3390/scipharm87040032>
- Salih OS, Ghareeb MM (2021) Formulation and in-vitro evaluation of thermosensitive ciprofloxacin HCL in-situ gel for local nasal infection. *International Journal of Drug Delivery Technology* 11(4): 1295–1301. <https://doi.org/10.25258/ijddt.11.4.29>
- Sneha R, Bajaj A, Londhe V, Babul N, Kao D (2017) Fabrication of topical metered dose film forming sprays for pain management. *European Journal of Pharmaceutical Sciences* 100: 132–141. <https://doi.org/10.1016/j.ejps.2017.01.004>
- Surab A, Alkurdi KA, Challacombe SJ, Tappuni AR (2023) Topical betamethasone and systemic colchicine for treatment of recurrent aphthous stomatitis: a randomised clinical trial. *BMC Oral Health* 23(1): 709. <https://doi.org/10.1186/s12903-023-03335-x>
- Swain GP, Patel S, Gandhi J, Shah P (2019) Development of moxifloxacin hydrochloride loaded in-situ gel for the treatment of periodontitis: in-vitro drug release study and antibacterial activity. *Journal of Oral Biology and Craniofacial Research* 9(3): 190–200. <https://doi.org/10.1016/j.jobcr.2019.04.001>
- Swami V, Chauhan DK, Santra P, Kothari K (2016) Design and development of solar pv-based power sprayer for agricultural use. *Annals of Arid Zone* 55(2): 51–57.
- Talal SH, Jabir SA, Al-kinani KK (2018) Investigating the effect of different grades and concentrations of ph-sensitive polymer on preparation and characterization of lidocaine hydrochloride as in situ gel buccal spray. *Asian Journal of Pharmaceutical and Clinical Research* 11(11): 401. <https://doi.org/10.22159/ajpcr.2018.v11i11.28492>
- Vardanyan RS, Hrubby VJ (2006) Corticosteroids. *Synthesis of Essential Drugs* 349–63. <https://doi.org/10.1016/B978-044452166-8/50027-3>
- Vijaybhaskar D, Shirsand S, Surampalli G (2022) A comparative physicochemical and pharmacological evaluation of dexamethasone sodium phosphate and betamethasone sodium phosphate mucoadhesive gels for the treatment of oral submucous fibrosis in rats. *Brazilian Journal of Pharmaceutical Sciences* 58. <https://doi.org/10.1590/s2175-97902022e20262>
- Vilasinee S, Sakdiset P, Puttarak P (2022) Development of oral microemulsion spray containing pentacyclic triterpenes-rich *Centella Asiatica* (L.) Urb. Extract for healing mouth ulcers. *Pharmaceutics* 14(11): 2531. <https://doi.org/10.3390/pharmaceutics14112531>
- Yuliia M, Herbina N, Dene L, Ivanauskas L, Bernatoniene J (2024) Development and evaluation of oromucosal spray formulation containing plant-derived compounds for the treatment of infectious and inflammatory diseases of the oral cavity. *Polymers* 16(18): 2649. <https://doi.org/10.3390/polym16182649>
- Zhang Y, Wu X, Li H, Du N, Song S, Hou W (2017) Preparation and characterization of betamethasone sodium phosphate intercalated layered double hydroxide liposome nanocomposites. *Colloids and surfaces. A: Physicochemical and Engineering Aspects* 529: 824–831. <https://doi.org/10.1016/j.colsurfa.2017.06.063>